

NATIONAL RADIO ASTRONOMY OBSERVATORY
ENGINEERING MEMO NO. 129

MEASURING THE SURFACE OF THE 140-FOOT; THE RESULTS

John W. Findlay

March 23, 1979

1. Introduction and Summary

Between October 17 and October 22, 1978, the stepping method was used to measure the shape of the 140-foot (42.7 m) telescope surface with the telescope fixed in the zenith position. This report summarizes the results of these measurements. Several earlier reports and memoranda have been written about the stepping method and the tests which have been made of its use. These reports are listed in Appendix 1, with a brief statement of the contents of each. The reports of the Engineering Division on the preparations for and conduct of the measurements are similarly referenced. Therefore, this present report will only briefly describe the method of measurement and will concentrate on a description of the results and a discussion of their meaning.

Two sets of measurements of the surface shape were made--referred to hereafter as Runs #1 and #2. Each measured 33 points along 68 radii. (The 4 radii which intersect the feed legs were omitted, so generally the radii were 5° apart.) Thus 2244 surface points were each measured twice. The actual measurement accuracy is hard to assess precisely. It was probably about 400 microns, but may have been as good as 250 microns. The measurements were taken under far from ideal conditions--the ambient air temperature varied within the range of 2°C to 25°C and each run took about 22 hours of measuring time to complete. In neither run were measurements continuous in time. Interruptions were caused by the surface icing, high wind and fatigue of the operators.

A best-fit surface was found for the results for each run. In making a best-fit, the focal length f (nominally 18288 mm) was adjusted, so also was the vertex, position and axis direction of the paraboloid. The reference system for the measurements was: O_z vertically upwards, O_x to the East and O_y to the North. Table 1 gives the best-fit surfaces derived from Runs 1 and 2. It will be noted that the RMS (mean = 1.263 mm) is close to the expected radio value, but the paraboloid axis shows a significantly different position between the two runs. These and other conclusions will be discussed later in the report.

Table 1. Results from Runs 1 and 2

Run No.	best-fit values for:						
	f mm	RMS mm	Move Vertex-mm			Rotate Axis	
			ΔX	ΔY	ΔZ	θ_x	θ_y
1	18273+1	1.235	19.0	-11.1	-0.48	-0.91 arc min	-1.62 arc min
2	18271+1	1.291	1.65	-7.7	-0.61	-0.62 arc min	-0.25 arc min

2. The Method of Measurement

The total measurement program can be subdivided into three tasks.

(a) Establish a reference (X,Y,Z) coordinate system which can be related to the physical structure of the telescope.

This was done in the following way. The origin 0 (Figure 1) was defined by the center of a steel sphere, itself located at the nominal vertex of the telescope. This sphere could (for convenience) be removed and replaced with accuracy. (See J. Ralston's Engineering Division (ED) Memo #121.)

The O_z direction was defined as being parallel to the local gravity vertical. The target radii were laid out by theodolite to be at 5° intervals, with radius #1 to the North and #19 to the East (see ED Memo #127). Since the

innermost ring of targets was to be used as the start point for the stepping bar for each radius, this ring had to be related in r and Z to 0. (r is the distance along a radius measured in the $[X,Y]$ plane.) This was done by the level and micrometer system described by Ralston in ED Memo #121.

(b) Establish the elevations of the end targets on each radius above and below a mean (X,Y) plane passing through them.

This step was made necessary since it could not be assumed that the telescope surface would remain fixed, with respect to gravity, throughout the measurements. However, if the elevations of the end targets were to be monitored at intervals during the measurements, it could be assumed that the relative positions of these end points would not change, and so these relative elevations could be used to correct for the telescope tilt as the various radii were measured. This assumption is discussed further later.

A Wild N-3 precision level was mounted about 1.5 m above the top of the Cassegrain house (see Figure A of ED Memo #127), and in this position it was at almost the same elevation as the outer ring of targets. At a small fixed distance beyond each of the outermost stepping targets on each radius a small optical target was fixed. The elevations of these optical targets (above and below a gravity-horizontal reference plane) were measured. All 68 targets were observed three times during Run #1. The closing values of those 68 values were not good (suggesting that the telescope surface was tilting by as much as 20 arc seconds during the hour or so it took to measure the levels). Thus during Run #2 only 12 optical targets every 30° of azimuth were measured. These level measures on the optical targets were used (as will be described later) to correct the stepping-bar runs along each radius for the tilt of the dish with respect to gravity. However, at this stage it is well to stress the point that these elevation measures of the optical targets give elevations above or below a plane, but that the elevation of this plane above the vertex 0 cannot be found from the Wild observations.

(c) Run the stepping bar along each radius.

There were 33 target locations for each radius, and the bar was placed sequentially between #1 and #2, #2 and #3, and so on. In Run #2, to save effort, the steps were made up radius #1, down #2 and so on. The data taking

was automatic (see ED Memo #122), ten values of the angle sensor were read and the mean value of θ_n (see Figure 1) and its RMS was recorded. Similarly, the mean of five values of the length sensor was also recorded. At the end of each radius the mean angle and length sensor voltages and the RMS of the angles in arc seconds were written onto the HP9825A cassette.

During Run #1 the radii were stepped in the following order:

1, 4, 7 70, repeat 1

2, 5, 8 71, repeat 2

3, 6, 9 72, repeat 3

During Run #2 the radii were stepped in sequence from 1 to 72. During each run the outside air temperature was recorded. For each step the following equations were used to relate the (θ, ℓ) values to (r, Z) values: --

$$\left. \begin{aligned} Z_{n+1} &= Z_n + \ell_n \sin \theta_n \\ r_{n+1} &= r_n + \ell_n \cos \theta_n \end{aligned} \right\} \text{---(1)}$$

3. The Form and Quality of the Raw Data.

(a) The measurements of the end targets.

Table 2 below lists the measurements made with the Wild level of the relative elevations of the optical targets at the ends of the radii. The closing error is the difference between the elevations of #1 target measured at the start and end of the set of observations.

Table 2. Measurements of the Optical Targets

Date or EDT of Measurement	No. of Targets Measured	Ambient Temp. °C	Closing Error in mm	Stepping Run No.
Oct. 17 1500-1600	68	6.0°	+0.10	1
Oct. 18 1315-1430	68	14.0°	-2.04	1
Oct. 18 1800-1900	68	11.5°	+1.23	1
Oct. 18 2330-2355	12	2.0°	-0.12	1
Oct. 19 2030-2045	12	11.5°	+0.18	1
Oct. 21 1455-1510	12	21.5°	+0.62	2
Oct. 21 1825-1840	12	16.0°	+0.22	2
Oct. 22 1525-1540	12	24.5°	+0.46	2

The various sets of edge measurements were fitted with a sine curve in order to find the departures of the edge target elevations from the best-fit plane passing through the targets. These measured departures (ΔZ) agreed fairly well from one set of measures to the next, but, as we shall see later, a significant difference could be seen between the ΔZ 's associated with measurements made during stepping Run #1 (Oct. 17-19) and Run #2 (Oct. 21-22).

The tilt of the best-fit plane through the edge values should be a measure of the tilt of the telescope reflector with respect to the gravity vertical. The tilt as thus determined (in arc seconds) and the azimuth of the line of greatest tilt downward (in degrees) are given in Table 3.

Table 3. The telescope tilt angle and direction determined from the edge target measures.

Date EDT of Measurements	Tilt Angle	Tilt Direction
Oct. 17 1500-1600	41 arc sec	+177°
Oct. 18 1315-1430	19 arc sec	+178°
Oct. 18 1800-1900	29 arc sec	+158°
Oct. 18 2330-2355	24 arc sec	+183°
Oct. 19 2030-2045	31 arc sec	+189°
Oct. 21 1455-1510	12 arc sec	+101°
Oct. 21 1825-1840	18 arc sec	+141°
Oct. 22 1525-1540	12 arc sec	+101°

Although the results shown in Table 3 show that the reflector surface remained fairly stable with respect to gravity, the movements are too large and variable to be used to fix the end-points of the stepping runs.

The results of the edge-target measures (the ΔZ values) do, however, show a significant overall change in shape of the telescope reflector as between stepping Runs #1 and #2. If we choose the first three sets* of ΔZ values as typical of stepping Run #1 and the last three as typical of stepping Run #2, we get the following results:

- (i) The mean ΔZ values agree well in the two sets of measures taken separately. (Figures 2(a) and 2(b) show the mean values and an error bar to show the RMS departure from the mean for each point.)

* Choosing all five sets as typical of stepping Run #1 gives a very similar result.

- (ii) There is a systematic change in reflector shape between October 17, 18, and 21, 22. Figure 2(c) shows this change. It is clear that the astigmatic behavior of the reflector is significantly altered. Since we shall use the curve 2(c) in later data reduction, we note here that the expression:

$$\{\Delta Z(1) - \Delta Z(2)\} = 1.105 \sin(10I + 77^\circ) \quad \text{—————(2)}$$

(I is the radius number) fits the points of 2(c) with an RMS difference of 128 microns.

(b) The stepping bar data.

The angle or length sensors each gave a ± 5 volts output when moved over their full range. Each was read by the digital voltmeter on the ± 10 volt range and so was recorded in the 9825A to the nearest 100 μV . This is equivalent to an angle change of 1.08 arc seconds and to a length change of 0.05 microns. (The length sensor was unnecessarily sensitive, but this did not matter in practice.)

Generally the angle measurement at any step showed an RMS value (printed directly by the computer) of less than 10 arc seconds. If a large RMS (>20 arc seconds) was read the step was reread.

At the end of Run #1 it seemed that some of the recorded lengths differed too much from the nominal ($\lambda = 650$ mm) step length. To check this, all length measures taken in Run #2 were checked against those recorded in the first run. A length value was accepted in Run #2 if it:

- (i) Fell within ± 250 microns of the nominal step length.
- (ii) If it did not satisfy (i) then it fell within ± 250 microns of the length value measured for that step in Run #1.
- (iii) In the event that neither (i) nor (ii) was satisfied, then the step was carefully repeated twice and the resulting value accepted.

Finally, in reducing the data, it was decided to use only Run #2 step lengths to reduce the stepping-bar data for both runs.

4. Reducing the Data

(a) Data format and storage.

The observed mean values of the tilt sensor voltage and the length sensor voltage were written onto a 9825A cassette tape. From this first cassette further working tapes were made. The measured elevations of the center ring or outer ring of targets were entered (by hand) onto these working tapes. The raw data on the working tapes was checked and edited to a standard format. Various other data--e.g., ambient air temperature and time--were also written onto the working tapes. As is explained in Appendix 2, data on a 9825A tape can, if needed, be read into the IBM 360.

(b) Data conversion.

Length sensor data was in the form of a voltage $V(\ell)$ which was between +5 volts. $V(\ell)$ was a measure of the difference between ℓ , the actual step length, and a nominal length. The conversions which apply to the two runs are:

$$\text{Run \#1 } \ell = 649.95 + 0.508 [V(\ell) - 1.6916] \text{ -----(3)}$$

$$\text{Run \#2 } \ell = 649.95 + 0.508 [V(\ell) - 0.0310] \text{ -----(4)}$$

where ℓ is in mm and $V(\ell)$ in volts.

As we have already noted, the length measures made in Run #2 were used to reduce both runs so that (4) only was used.

The angle sensor was calibrated on July 13, 1978. A 12-inch inductosyn was used as an angle-measuring device, over the range + 14.5°. The inductosyn has a least significant bit corresponding to an angle of 1.6 arc seconds. The inductosyn angle θ was found to be related to the tilt sensor voltage V by the relation:

$$\sin \theta = (0.007214-V) \times 0.0500464 - 0.95 \times 10^{-6} \times V^2 \text{ -----(5)}$$

The RMS value for the difference between the inductosyn angle and θ derived from (5) was 0.92 arc seconds. The manufacturer gave

$$\sin \theta = (0.0071-V) \times 0.0501036 \text{ -----(6)}$$

as a calibration but agrees that a V^2 term is needed for high accuracy.

Thus (5) was used throughout to convert sensor voltages to tilt angles. Since the sensor has a small temperature coefficient of gain, amounting to

0.005% of the reading per °F, a corresponding adjustment was made to the sensor readings under the assumption that the sensor temperature followed the ambient air. This correction was small.

(c) The individual profiles.

The raw data for tilt angle, derived from (5) and step length from (4) were used to give the profiles along each radius in the form of (Z, r) values. The steps in this process were as follows:

(i) The starting ring of targets

The (Z,r) value for target #1, which was on the inner ring of targets, was derived from the values for this ring measured by the method developed by Ralston (Memo #127 paragraph 3(c)). As with the outer target ring, a best-fit plane was passed through the inner ring points. The Z-values assigned to these inner ring targets were 33.94 mm + the measured departures from the best-fit plane. The r-value for all points was 1575.77 mm.

(ii) Stepping and edge-fitting

For each step of length ℓ and angle θ (derived from (5) and corrected for ambient temperature) the increments in r and Z were computed from:

$$\left. \begin{aligned} \Delta r &= \ell \cos (\theta - \theta_0) \\ \Delta Z &= \ell \sin (\theta - \theta_0) \end{aligned} \right\} \text{-----} (7)$$

In (7) the angle θ_0 is a combination of the unknown zero-point angle of the bar and inclinometer and the small but unknown tilt with respect to gravity of the radius being measured. This θ_0 was adjusted for each radius so that when the computations reached the (r,Z) value for the outer target the actual Z value was consistent with the value measured for that radius as described already in 3(a).

The above statement requires further explanation. For a given radius and a chosen θ_0 the application of (7) to all steps out to the end yields a set of (r,Z) values. Let us now choose a focal-length f for this radius and for each (r,Z) value compute the difference D(Z) where

$$D(Z) = Z - r^2/4f \text{-----} (8)$$

We now adjust θ_0 until D(Z) for the edge target is equal to the ΔZ derived as described in 3(a).

In practice, all the first results of Runs #1 and #2 were reduced in this way, with the design focal length (18288 mm) used for f in (8). The difference in reduction between Runs #1 and #2 lay in the use of equation (2) to modify all the edge $\Delta(Z)$ values used in Run #2 as compared to Run #1. This change was made because there is good evidence that the general shape of the dish did in fact change between Runs #1 and #2, yet we only had available the $\Delta(Z)$ edge measures for all radii made during Run #1.

(iii) Mapping and best-fitting

The (r,Z) values for each run were next converted, using the known angles of the radii, to (X,Y,Z) values. In this form they could be used as input to a best-fitting program (RMS 2244) which chose the paraboloid of best-fit. In doing this the focal length was adjusted; so also was the vertex position and axis direction of the paraboloid. Since a value of f had already been chosen (in equation (8)), it was necessary to carry the best-fit process back to the point where different values of f were used in (8) and the programs run until a minimum value for the RMS departure of the points from the best-fit surface was found. Figure 3 is an example of the results of this best-fit analysis. It shows for Run #1 (both runs show very similar results) how the final RMS alters as various values for f are chosen in (8) and then RMS 2244 run to give the final best-fit.

(d) The contour maps

After the data had been processed by RMS 2244, it was in the form of (X,Y,Z) points which could be entered into the standard Calcomp contour plotting program. (Two programs are needed, PLT 140A and PLT 140B.) Plots from this program, with a contour interval of 1 mm, are shown in Figures 4(a) and 4(b). These plots also show the locations (+) of all measured points and the outlines of the surface panels.

5. Discussion of the Results

Two general conclusions can be drawn from the results of the measurements. First, it appears that the reflector surface is quite close in shape to the design paraboloid. The values in Table 1 for f are well within the values expected from the original measurements (DS Kennedy) of the surface panels and for the adjustment of the panels on the telescope. The RMS values

(mean 1.263 mm) would lead us to expect an aperture efficiency of about 45% at $\lambda = 3$ cm--a result which is reasonably close to measured values.

The second conclusion is that there appears to be significant differences between the surface shapes measured in Runs #1 and #2. We will discuss this in more detail in what follows.

(a) The systematic differences

As has been shown in 3(a), the edge target measures show a systematic change of shape between Runs #1 and #2. We should repeat that these edge-target measures were made in the simplest way, using only a precise Wild N-3 level. We have shown in Figures 2(a), 2(b) and 2(c) not only the apparent consistency of the measurements but also the systematic change. Another way of showing this is to look at the astigmatism the edge measures show by fitting a sine curve with two complete periods around the dish. Such a curve is, for Runs #1 and #2 (or for Figures 2(a) and 2(b)),

$$\left. \begin{array}{l} \text{Run \#1 } \Delta Z = 1.229 \sin (10I + 45) \\ \text{Run \#2 } \Delta Z = 0.659 \sin (10I - 19), \end{array} \right\} \text{-----(9)}$$

where ΔZ is in mm and I is the radius number.

The results of (9) show the dish was less astigmatic during Run #2 than during Run #1, and that the radius of no astigmatism moved 64° around the dish between the runs. Lastly, it can be noted that during the Run #1 edge measures (Table 2) the average air temperature was 10.5°C and during Run #2 it was 20.7°C .

(b) Unsystematic differences

A study of the differences between Run #1 and Run #2 should, if the telescope remained stable in shape, give a good estimate of the accuracy of the measurement system. For this reason, the point-by-point differences between the two runs were studied. This was done in two ways for the measured Z values before the results had been run through the best-fit program.

First, for each radius the 32 values of Z from the two runs were compared. As an estimate of the average difference between the two sets of Z values, the quantity R was computed:

$$R^2 = \frac{1}{32} \sum_{i=1}^{32} \left\{ Z^{(1)}_i - Z^{(2)}_i \right\}^2 \text{-----(10)}$$

where $Z(1)_i$, $Z(2)_i$ are the measured Z values in Run #1 and Run #2 for the i^{th} point along the radius.

Figure 5 shows how R varies with the radius being measured, and it suggests that, for some reason, large R-values are associated with radii 1 through 5 and 57 to about 65. Before discussing this further, we examine the differences between Runs #1 and #2 in another way. For every measured point on every radius the differences between the Run #1 and Run #2 Z-values were computed. (Again, these were the Z-values before the best-fit operation.) Then, in Figure 6, we have plotted a contour map of these differences in Z-values between the two runs. (In the sense $\delta Z = \text{Run \#2} - \text{Run \#1}$.) The concentration of large Z-differences in two areas of the dish should be noted.

(c) Explanations of the unsystematic differences

We can provide no firm reason to explain the differences between Runs #1 and #2, and so we will list and comment on some possibilities.

(i) Measurement errors

It is not possible to rule out this as the reason, but the following evidence seems to make it unlikely. First, measurements on Runs #1 and #2 agreed in some cases reasonably well (see the large areas of Figure 6 where δZ lies between ± 1 mm). Second, Run #2 was done for radii 1, 2, 3 in order while #1 was done 1, 4, 7; 2, 5, 8; 3, 6, 9 It seems unlikely that measurement errors in Run #1 could be responsible, but errors in #2 are possible. Third, it is possible to compare results on radius #54 with measurements made on one of four radii on June 7 and 8, 1978 (see Engineering Memo #124). The radii measured were not identical. They were 1.5° apart in azimuth. Figure 7 shows the mean results in June (3 runs) and in the present measurements (2 runs). The agreement is good.

(ii) Effects of temperature

There were quite large (up to about 23°C) ambient temperature differences between runs over the same radius. However, it is not possible in general to relate these temperature differences directly to observed differences between the Z-values. To make this point more clear, we have compared the 68 R-values derived from (10) with the corresponding $|\Delta T|$ values, where $|\Delta T|$ is the modulus of the difference in temperature between the times the

measurements were made. No correlation is obvious on a plot of R against $|\Delta T|$ and the correlation coefficient between the 68 pairs of values is 0.08, or essentially zero.

However, if we wish to examine the possibility that radii in the 1 to 8 and 55-65 number range were sensitive to temperature, we can consider Table 4, which lists the R-values (Equation (10)) and $\Delta T^\circ\text{C}$ (in the sense Run #2 - Run #1), for these radii.

Table 4. Values of R and ΔT for selected radii.

Radius #	Date in October of Measurement and $T^\circ\text{C}$				$\Delta T^\circ\text{C}$	R_{mm}
1	17th	6°	21st	17.0°	11.0°	1.026
2	18th	13.5°	"	17.3°	3.8°	1.365
3	19th	12.0°	"	17.6°	5.6°	2.774
4	17th	6°	"	18.0°	12.0°	1.487
5	18th	12.5°	"	19.0°	6.5°	1.703
6	19th	11.7°	"	19.3°	7.6°	1.100
7	17th	6.1°	"	19.7°	13.6°	.430
8	18th	11.8°	"	20.0°	8.2°	1.307
55	18th	16.3°	22nd	25.0°	8.7°	.639
56	18th	2.0°	"	25.0°	23.0°	.637
57	19th	9.9°	"	25.0°	15.1°	1.445
58	18th	16.4°	"	25.0°	8.6°	.587
59	18th	2.0°	"	25.0°	23.0°	.601
60	19th	9.9°	"	24.9°	15.0°	2.459
61	18th	16.5°	"	24.3°	7.8°	1.602
62	18th	2.0°	"	23.7°	21.7°	1.434
63	19th	9.7°	"	23.0°	13.3°	.953
65	18th	2.5°	"	22.3°	19.8°	3.285

There seems no evidence in this Table that the large R-values and large ΔT values are closely related. The only point appears to be that all the fairly large or large R-values are associated with positive ΔT 's. This says that generally Run #2 was made at a considerably higher ambient temperature than Run #1.

(d) Estimated measuring accuracy

An estimate of the measuring accuracy can be made by using an expression such as (10) to derive R. The values of R will include effects of measurement

inaccuracy and effects of telescope shape changes between the runs. Also, R is derived from the difference in Z values between Runs #1 and #2, where half the difference might be more suitable. If we chose (R/2) as an estimate of the measuring accuracy we get:

For all 68 radii $R/2 = 422$ microns

For radii 6 through 55 $R/2 = 252$ microns

We may thus roughly estimate the measuring accuracy as 400 microns, with the possibility that it was as low as 250 microns.

6. Conclusion

Although both sets of measurements show that the telescope surface shape is close to its design, the parts of the surface which show different shapes between the runs have not been explained. Before further work is done on the telescope, a program of study of these doubtful areas has been started in the hope that the results will help clarify the differences.

Appendix 1
Bibliography

(a) 25-Meter Telescope Memos

No. 68 of Jan. 26, 1977, describes the method of measuring by stepping.
Nos. 70, 82, and 95 further describe the inclinometer, the stepping
bar and tests of the system.

No. 94 describes the first trial, over one radius, of the method on
the 140-foot.

(b) Engineering Memos

No. 121 of March 14, 1978, describes the various things to be done
to prepare the telescope for measurement of 48 radii.

Nos. 122, 123 and 124 describe the proposed survey, the method of
data taking and the test results obtained in June, 1978, on four
radii.

No. 127 describes the engineering and practical aspects of the present
survey.

Appendix 2

A Note on Writing Data from the HP9825A to the IBM 360/50

In the tests of the curvature-measuring cart (Electronics Division Internal Report #176), the data from a 14-bit A/D converter was written onto a 7-track tape at 556 BPI by a Digidata Stepping Recorder. The interface to do this was designed and built by D. Schiebel. Since the HP9825A can be programmed to present any number in its store as a 16-bit binary number at its output, it seemed likely that it might be possible to write 7-track tape from the 9825A. D. Schiebel made the necessary changes to the interface he built, and a fairly simple program can now write from the HP9825A storage (and so from a cassette) onto a 7-track tape which, in turn, can be read into the IBM 360.

In the present work the first stages of data reduction were done in the 9825A, and then the 33 pairs of (r,Z) values for each radius were transferred to the IBM 360. The r and Z values were each scaled in such a way that no significant accuracy was lost despite the limitation of a 16-bit word length. The method was fully tested, and details are available from D. Schiebel or from J. Findlay.

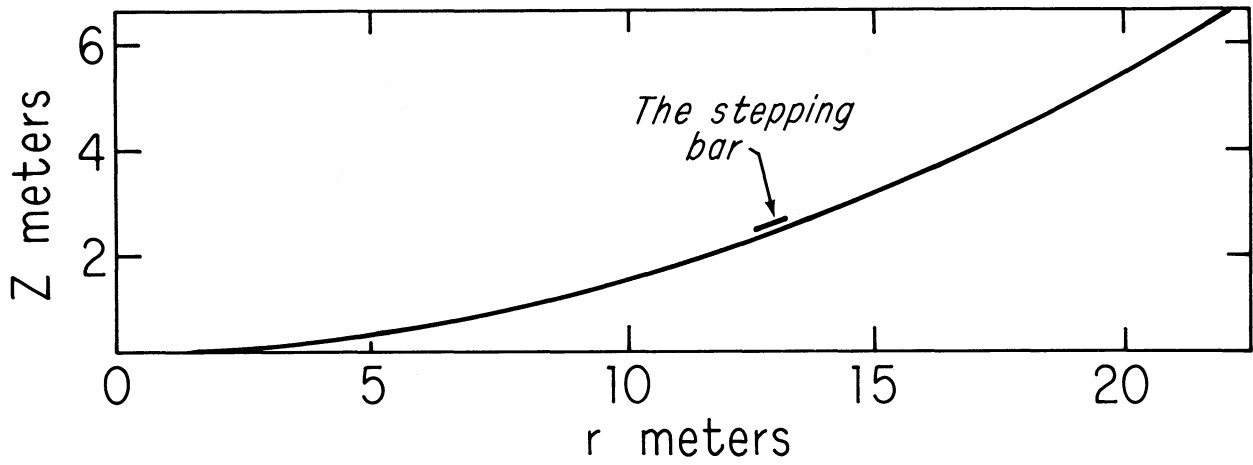


Fig. 1(a) The Reflector and Stepping Bar, to scale

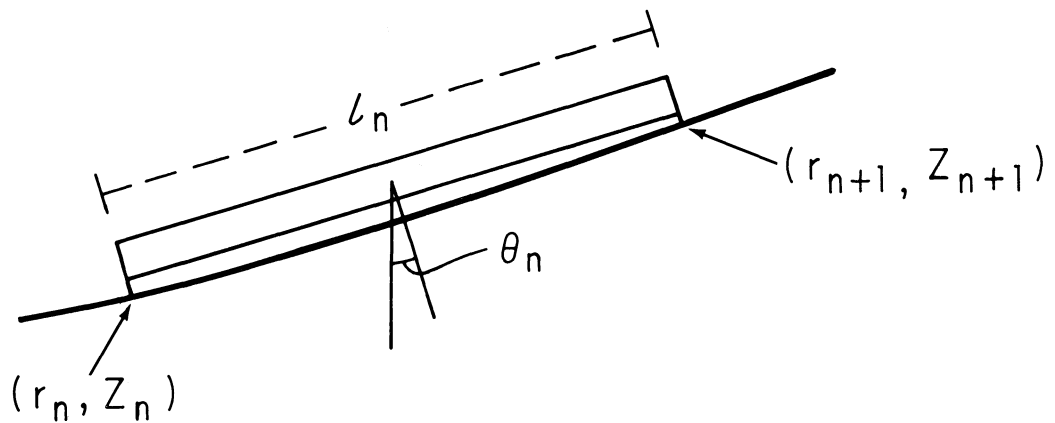


Fig. 1(b) The Bar on Step #n

Fig. 1 Measuring by Stepping

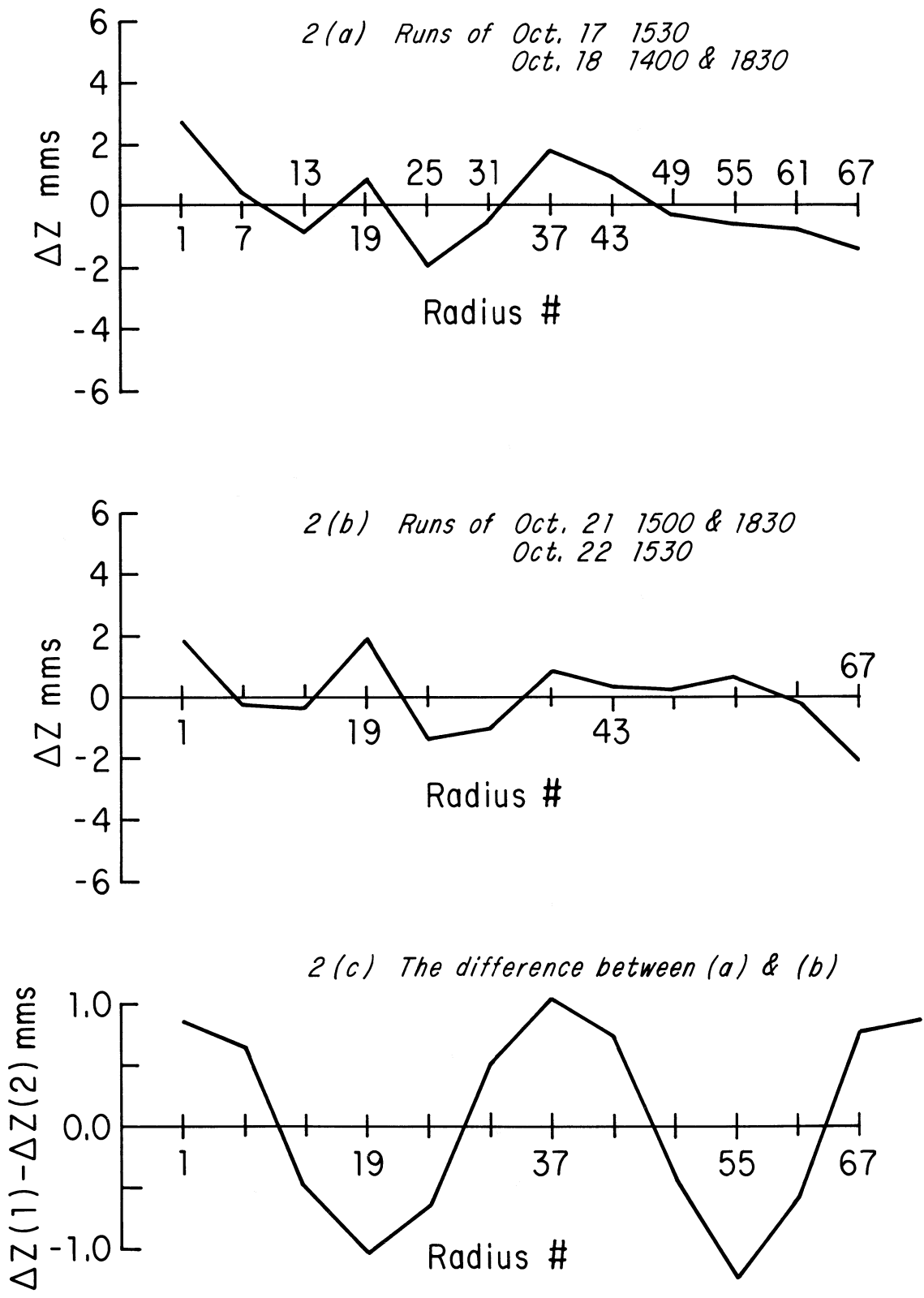


Fig. 2 The Measurements of the Edge Targets

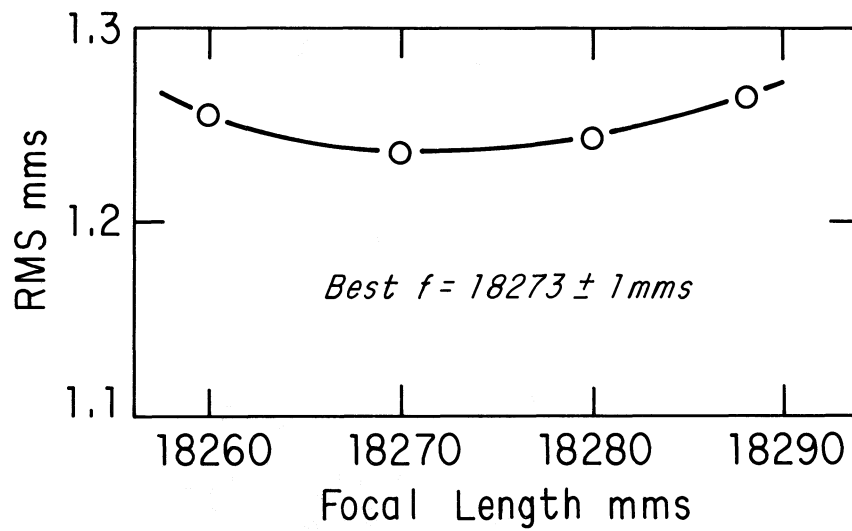


Fig. 3 The RMS of the Best-Fit Surface for Run # 1 as the Focal Length is Changed

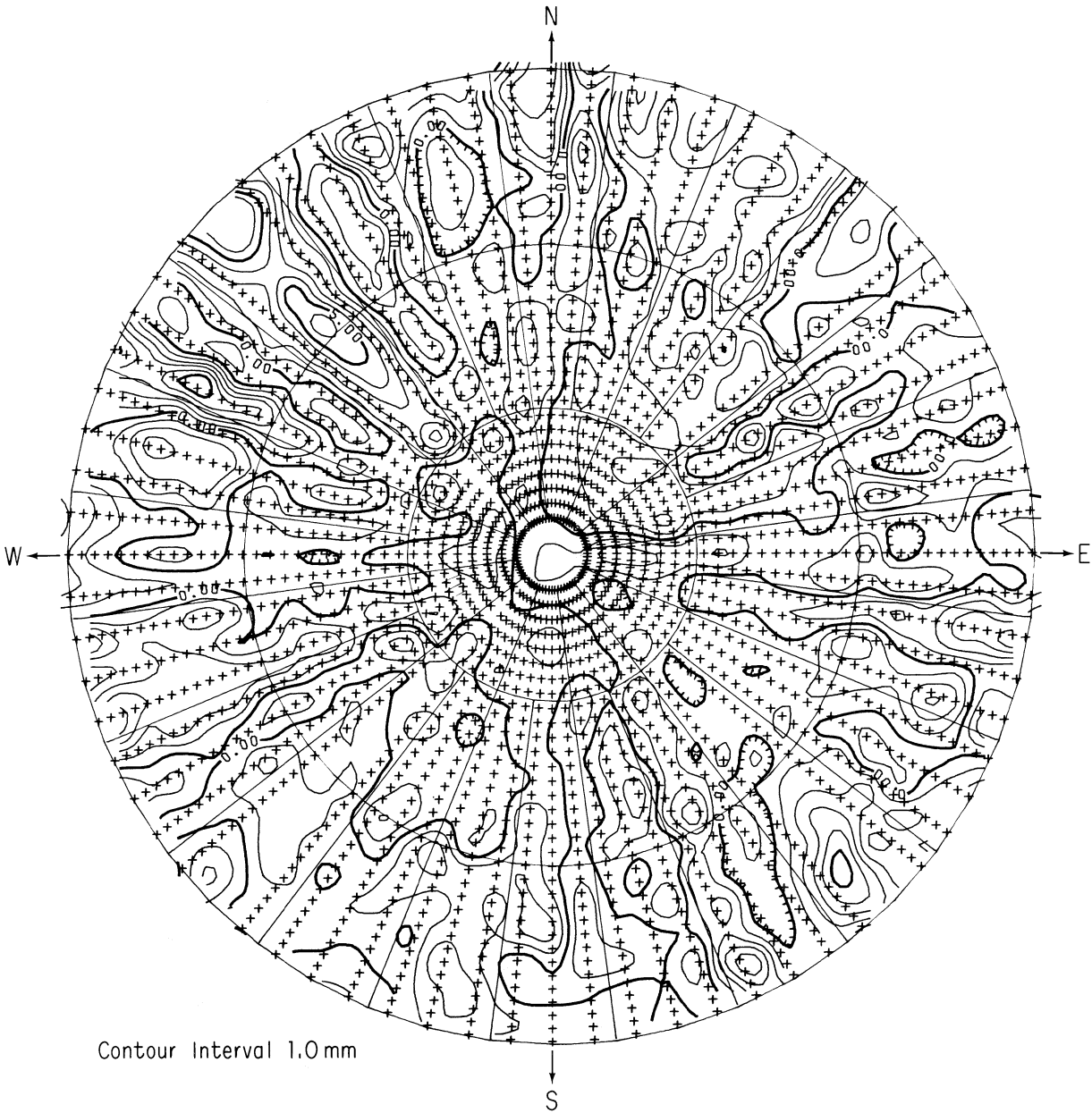


Fig. 4(a) The 140-Foot, Run # 1 -- Departures from the Best-Fit Paraboloid

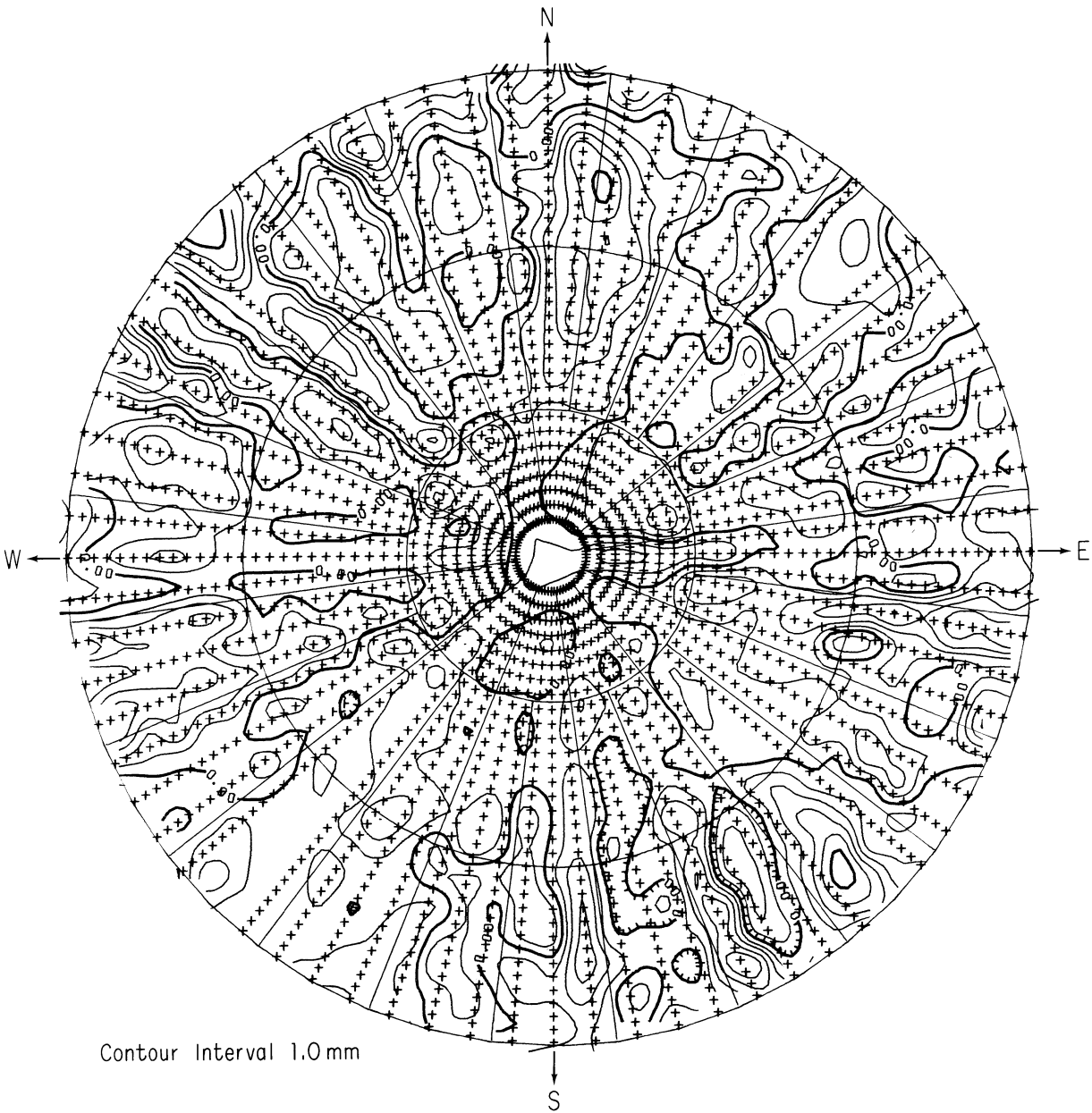


Fig. 4(b) The 140-Foot, Run # 2 -- Departures from the Best-Fit Paraboloid

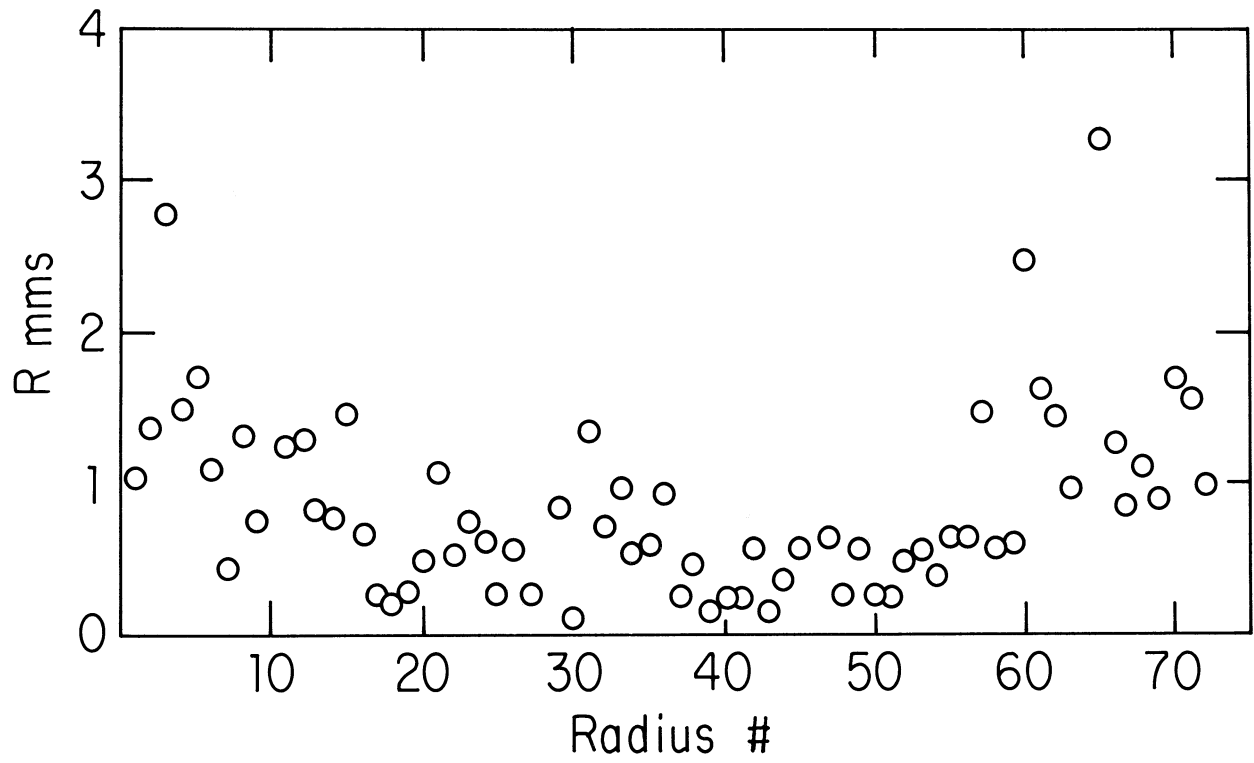


Fig. 5 The R Values as a Function of Radius

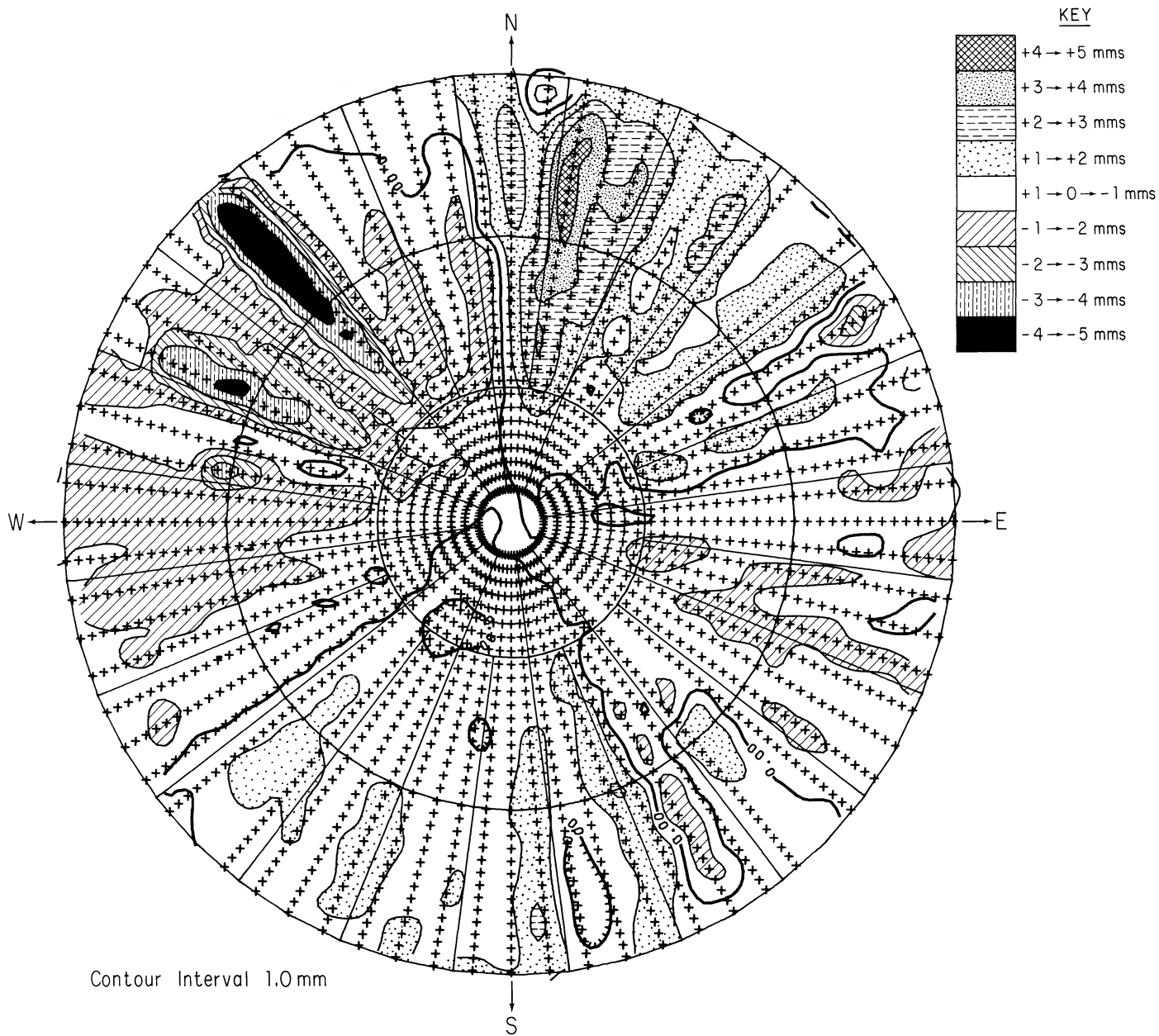


Fig. 6 Differences in Z Values, (Run # 2 - Run # 1)

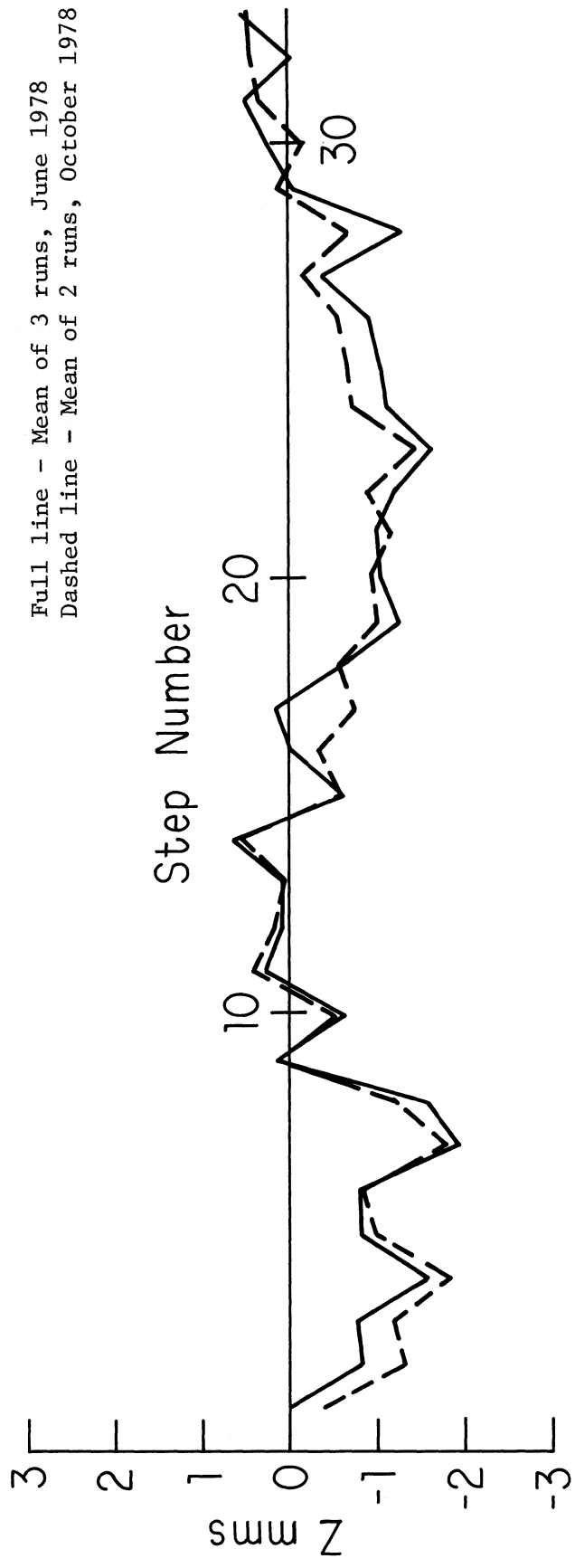


Fig. 7 Measurements over Two Radii 1.5° Apart in Azimuth